# Column collapse and generation of pyroclastic density currents during the A.D. 79 eruption of Vesuvius: The role of pyroclast density

Thomas Shea[1], Lucia Gurioli[2], Bruce F. Houghton[1], Raffaello Cioni[3], and Katharine V. Cashman[4]
[1]Department of Geology and Geophysics, University of Hawaii, Honolulu, Hawaii 96822, USA
[2]Université Blaise Pascal, Laboratoire Magmas et Volcans, 63000 Clermont-Ferrand, France
[3]Dipartimento di Scienze della Terra, Università degli Studi di Cagliari, 01927 Cagliari, Italy
[4]Department of Geological Sciences, University of Oregon, Eugene, Oregon 97403, USA

## ABSTRACT

**The Plinian columns formed during the magmatic phase of the A.D. 79 eruption of Vesuvius alternated several times between fully stable, buoyantly rising regimes and unstable regimes of partial or total collapse. Six pyroclastic density currents (PDCs) were produced during unstable regimes, and ultimately caused the destruction of Roman towns around the volcano. Through new measurements of juvenile clast density and estimations of ascent parameters, we show that four partial collapses were likely triggered by increases in the abundance of dense juvenile clasts within the eruptive column. In contrast, the total collapse probably occurred in response to an increase in the wall-rock content injected into the plume during a progressive widening of the conduit. A sixth low-energy, small collapse resulted from high abundances in both dense juvenile clasts and wall-rock material. Simulations of eruption column behavior already account for the effects of variations in conduit radius, mass discharge rate, and particle size, but have yet to include variable clast density and wall-rock abundance that cause temporal variations in plume density. Our results suggest that both parameters can exert a significant control on the potential for generation of PDCs.**

## INTRODUCTION

Pyroclastic density currents (PDCs) can be generated by collapsing eruption columns during highly explosive eruptions (e.g., Wilson et al., 1980), and are among the deadliest hazards for populations living around volcanoes. Four main types of eruptive column regimes are typically recognized in the literature (e.g., Neri et al., 2003). (1) Fully stable or convective columns rise buoyantly due to an efficient entrainment of atmospheric air into the hot gas and particle mixture, and spread laterally when neutral buoyancy is reached. (2) The partial collapse regime occurs when a margin of the column collapses downward. (3) The total collapse regime involves its full destabilization. Partial and total collapse regimes often generate directed or radially dispersed PDCs. (4) A fourth type of behavior (termed the "boil-over" or "fountain collapse" regime) occurs when the ejected mixture is unable to mix efficiently with the surrounding atmosphere and spreads laterally rather than convecting upward (e.g., Clarke et al., 2002). In the past 40 yr, volcanologists have made extensive use of physical and numerical models to predict column behavior and the formation of PDCs. Early pseudogas numerical models of column dynamics suggested that fully buoyant plumes can collapse following increases in mass discharge rate (MDR) and/or vent radius, or decreases in exit velocity and/or initial dissolved water content (e.g., Wilson et al., 1980). In more recent numerical simulations, partially or fully collapsing columns have been generated by using particles of multiple sizes (i.e., where larger particles segregate from the main plume; Clarke et al., 2002), by decreasing the connectivity of gas bubbles within the magma at the fragmentation level (Kaminski and Jaupart, 2001), or by increasing microlite content (Neri et al., 2003).

While these plume collapse conditions may apply to some eruptions, it is unlikely that they can be invoked for the A.D. 79 eruption of Vesuvius, which switched at least six times between fully convective, partially collapsing, fully collapsing, and boiling-over behaviors. In this paper we explore a new alternative hypothesis: could the shifts in column dynamics have been produced by fluctuations in the density of the eruptive plume? The density of erupted juvenile clasts and the abundance of wall-rock material within the column are two factors that strongly influence column density. However, they have never been considered as transient variables within numerical models, even though they may play an important part in modifying plume dynamics. After a brief summary of the shifts in column behavior and the production of PDCs during the A.D. 79 eruption, we provide new density measurements made on pumice from both PDC and fall units along with wall-rock abundance throughout the eruptive sequence. We complement those measurements with new and existing calculations of physical eruptive parameters that could also have affected the eruptive plume, such as conduit radius, magma discharge rate, and magma decompression rate. We argue that the important transitions in column behavior can be linked to two main transient factors acting in concert: juvenile pumice density and wall-rock abundance related to an enlargement of the conduit-vent system.

## GENERATION OF PDCS DURING THE A.D. 79 VESUVIUS ERUPTION

In A.D. 79, Vesuvius produced the most lethal explosive eruption of its past 3000 yr of activity. This eruption lasted more than 20 h and deposited >3 km$^3$ of ejecta (dense rock equivalent; Cioni et al., 1992) around the volcano (Fig. 1A). During the eruption, the feeding magma shifted from a phonolite (termed white magma) to a tephriphonolite (gray magma) composition, emitting first white, then gray pumice (Lirer et al., 1973; Sigurdsson et al., 1985). The eruptive column switched at least six times from fully buoyant to partially collapsing, fully collapsing, and boil-over conditions (Cioni et al., 2004), generating alternations of fall and PDC deposits, termed eruptive units EU1–EU8 (Cioni et al., 1992). Herein

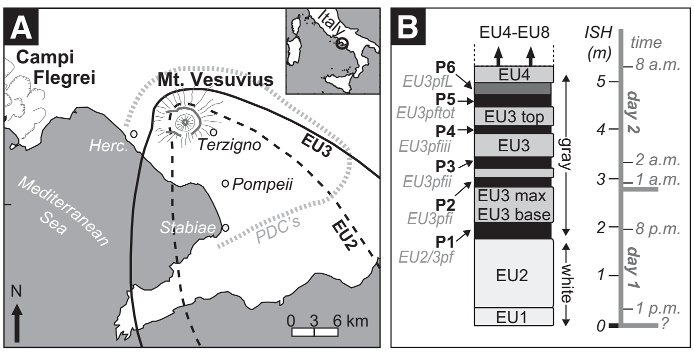


**Figure 1. A: Map of Vesuvius (Italy) area with locations of Roman settlements in A.D. 79. Fall 10 cm isopachs for eruptive units EU2 and EU3 are shown, along with extent of pyroclastic density current deposits (PDC) (cf. Gurioli et al., 2005). Herc.—Herculaneum. B: Simplified stratigraphy of magmatic phase of A.D. 79 eruption, with eruption timeline. Nomenclature of Cioni et al. (2004) is shown in gray below P1–P6. ISH—idealized stratigraphic height (m) if all units could be observed at one location.**

© 2011 Geological Society of America. For permission to copy, contact Copyright Permissions, GSA, or editing@geosociety.org.
*Geology*, July 2011; v. 39; no. 7; p. 695–698; doi:10.1130/G32092.1; 3 figures; Data Repository item 2011213.

we use the same EU nomenclature for fall samples, but designate the six PDCs investigated as P1 to P6 for simplicity (Fig. 1B).

An initial short-lived phreatomagmatic phase (EU1) was followed by a magmatic phase that lasted ~18 h (EU2–EU3; Fig. 1B). The eruption of EU2 pumice produced a stable Plinian column that rose to ~25 km in the atmosphere (Carey and Sigurdsson, 1987). The transition from white to gray magma (EU2 to EU3) was marked by the first partial collapse and the production of the first PDC (P1), which killed most inhabitants of Terzigno and Herculaneum. A fully convective column was then restored for the first 3–4 h of gray pumice fall (EU3base–EU3max). Subsequently, the column shifted back to a transitional behavior, partially collapsing and generating three PDCs (P2, P3, and P4; Fig. 1B). P2 was produced during the peak in MDR (EU3max; Fig. 1B), which was inferred from column height calculations by Carey and Sigurdsson (1987), while P3 and P4 were generated as MDR declined. The eruptive plume fully collapsed shortly after, forming a radially dispersed PDC (P5) that partly destroyed Herculaneum and reached Pompeii (Gurioli et al., 2002). The main magmatic phase of the eruption ended with the production of a boil-over that generated a poorly dispersed, massive, wall-rock–rich PDC (Cioni et al., 2004; P6). In subsequent phases of the eruption, the chamber and conduit regions progressively collapsed, and underground water may have interacted again with the rising magma. This resulted in a global shift toward phreatomagmatic activity (EU4–EU8). At least five more PDCs were produced, completing the destruction of Pompeii and taking the lives of all survivors around Vesuvius (Cioni et al., 1992, 2004). This paper focuses only on the six major PDCs generated during the magmatic phase of the eruption, P1 through P6. In the following, we compare interbedded PDC and fall samples in terms of juvenile clast density, wall-rock abundance, and other eruption parameters.

## METHODS

### Pumice Density and Wall-Rock Contents

Pumice density data were already available for several fall samples (cf. Gurioli et al., 2005). We collected ~100 additional 16–32 mm juvenile pumice clasts for each PDC unit and measured their densities. Density histograms were produced and clasts representative of the mode, the low, and the high end members were chosen to undergo vesicle number density measurements (Table DR1 in the GSA Data Repository[1]).

We compiled wall-rock abundances for EU1 to EU4 (from the studies of Lirer et al., 1973; Barberi et al., 1989; Gurioli et al., 2002; Cioni et al., 2004) (Table DR2) and converted from weight to volume fraction to account for the lower pumice densities compared to wall rock ($\rho_{wall} > 2.4$ g cm$^{-3}$; Table DR2).

### Decompression Rate and Conduit Radius Calculations

Estimates of magma decompression rates can be obtained directly from measurements of vesicle number densities (Toramaru, 2006). Vesicle number densities per unit volume melt ($N_V$) were derived using thin sections made from selected clasts via the FOAMS (Fast Object Measurement and Acquisition System) code (Shea et al., 2010a). The value of $N_V$ depends strongly on magma properties such as surface tension $\sigma$ (melt bubble and crystal bubble) and volatile diffusivity $D$, as well as on the time available for vesicles to nucleate (i.e., decompression rate $dP/dt$). In turn, if magma properties are known, vesicle number densities can be translated directly into estimates of decompression rates. As in Shea et al. (2010b), this conversion is achieved by using the equation presented in Toramaru (2006):

$$N_{\mathrm{V\,calc}} = 34X_0\left(\frac{16\pi\sigma^3}{3kTP_0^2}\right)^{-2}\left(\frac{\Omega_{\mathrm{M}}P_0}{kT}\right)^{-\frac{1}{4}}\left(\frac{kTX_0DP_0}{4\sigma^2\left|\frac{dP}{dt}\right|}\right)^{-\frac{3}{2}}, \qquad (1)$$

where $X_0$ is the water concentration at initial pressure, $k$ is the Boltzmann constant, $\Omega_M$ is the volume of water molecules in the melt, $P_0$ is the initial pressure, and $T$ is temperature. (For the detailed procedure used to obtain $dP/dt$, see the Data Repository.)

Estimates of conduit diameter variations during the magmatic phase were calculated in two ways. First, the conduit dimensions at depth (i.e., >2 km below Vesuvius) were calculated by assuming that the mass of wall rock with deep origins (i.e., carbonates; Barberi et al., 1989) measured within fall deposits correspond approximately to the mass of the conduit that was removed below volcanic eruptives in the area during the eruption. The mass of deep-seated wall rocks was thus integrated over four fall units (EU1, EU2, EU3base, EU3top) sampled at 24 sites at locations 5–90 km away from the vent. The conduit diameter was then obtained from integration of this mass along a cylindrical conduit (Table DR3). Second estimates of conduit diameter were derived using the conduit model ConFlow (Mastin and Ghiorso, 2000) using constraints given by the decompression rates (this study), and the MDR from Carey and Sigurdsson (1987) (see Table DR3 for input values).

## RESULTS

### Density Variations During the A.D. 79 Eruption

Density measurements obtained for both fall and PDC samples reveal several key features of the A.D. 79 magmatic phase. Although pyroclast density data are usually shown as distributions (Shea et al., 2010a, and references therein), we opt to group juvenile clast densities into three broad categories: low ($\rho$ < 800 kg m$^{-3}$), mean ($\rho$ = 800–1000 kg m$^{-3}$), and high ($\rho$ > 1000 kg m$^{-3}$). These cutoffs were chosen because modes from the density distribution of most fall samples are within the low-density group, and modes of most PDCs are within the mean- and high-density categories.

Overall, there is a tendency for the fraction of dense juvenile clasts present in PDC deposits to increase abruptly compared to preceding fall units (Fig. 2). The fraction of mean plus dense clasts (i.e., $\rho$ > 800 kg m$^{-3}$) reaches 70%–98% of total clasts in all PDCs (excluding P5), whereas most fall phases have values between 0% and 35%. P5 has intermediate values, with 55% clasts with $\rho$ > 800 kg m$^{-3}$. Note that the EU3base fall

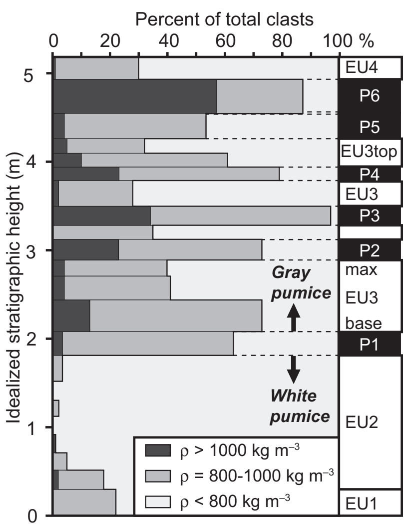


**Figure 2. A: Variations in density displayed as fractions of low-, medium-, and high-density pumice. Abrupt increases in pumice density are associated with partial collapses P1, P2, P3, P4, and P6. EU—eruptive unit.**

[1]GSA Data Repository item 2011213, supplementary text and Tables DR–DR3, is available online at www.geosociety.org/pubs/ft2011.htm, or on request from editing@geosociety.org or Documents Secretary, GSA, P.O. Box 9140, Boulder, CO 80301, USA.

deposit is also fairly rich in dense clasts, and thus departs slightly from the propensity of fall layers to contain mostly light pumice.

### Evolution of Decompression Rate

Decompression rates calculated using bubble number densities of low, modal, and high density clasts are, on average, much lower for the white magma than those obtained for the gray magma (0.4–1.2 MPa $s^{-1}$ and 0.6–12.8 MPa $s^{-1}$, respectively; Fig. 3A). Note that for P2, decompression rates calculated using magma properties intermediate between white and gray compositions are between values of EU2 and EU3base. Inferred decompression rates are initially low at ~0.5 MPa $s^{-1}$ during EU1, and increase to ~1.1 MPa $s^{-1}$ during EU2. Much higher inferred decompression rates of 2.3–7.8 MPa $s^{-1}$ are reached during initial eruption of gray magma (EU3base). Peak values of ~12.8 MPa $s^{-1}$ are calculated for the low-density pumice of P5, while P6 suggests diminished rates of decompression.

### Wall-Rock Abundances

The EU1 deposits contain a high proportion of wall rocks (~45 vol%; Fig. 3B; Table DR3) associated with the involvement of non-negligible amounts of external water and with the initial formation of the conduit system (≤10 m in diameter; Fig. 3C). Once a larger conduit system was formed (~40 m in diameter; Table DR3) and the eruption no longer involved external water (EU2 to P2), the fraction of wall rocks found within the deposits decreased significantly (~3–10 vol%). Wall-rock abundances remain low within deposits P2 to P4, and increase again during P5 and P6 (~15 and 65 vol%, respectively), likely reflecting widening of the conduit. By EU3top time, the conduit had been significantly eroded, and, by EU4 time, the upper portions of the reservoir regions had begun collapsing (e.g., Cioni et al., 1992), injecting more wall-rock material into the eruptive plume (~25–30 vol% within EU4).

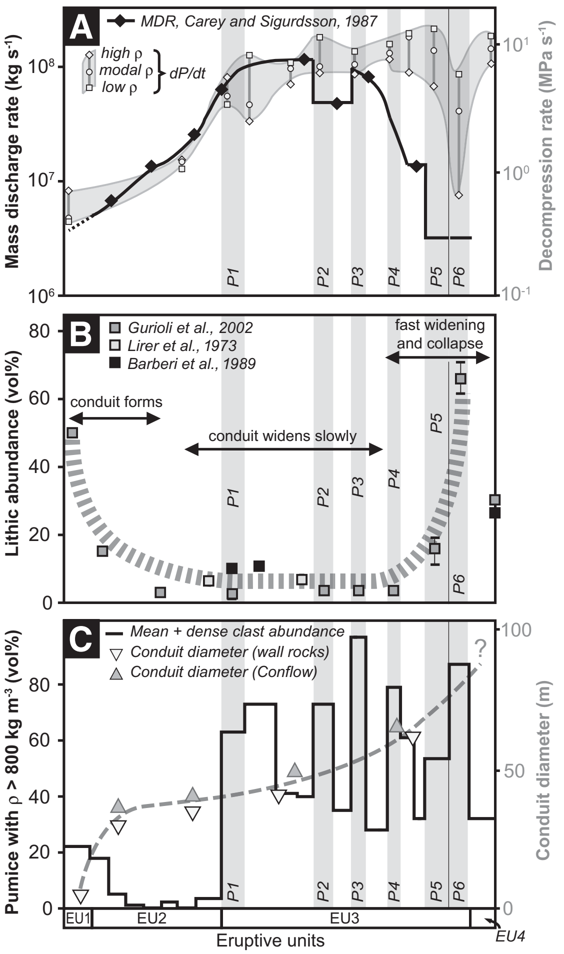


**Figure 3. Factors inducing column collapses during magmatic phase of A.D. 79 eruption. A: Variations in mass discharge rate (MDR; Carey and Sigurdsson 1987) and decompression rate *dP/dt* variations (see text). B: Abundance of wall rocks within deposits from various phases of A.D. 79 eruption from eruptive units EU1–EU4. C: Evolution of abundance of mean and dense clasts, and changes in conduit diameter from different sources (ConFlow simulations and mass of wall rock). Diameter for EU4 is speculative.**

## IMPORTANCE OF PYROCLAST DENSITY IN DRIVING TRANSITIONS FROM STABLE TO COLLAPSING ERUPTIVE COLUMNS

During the magmatic phase of the eruption, the column collapsed at least six times. Here we link some of the factors proposed as causes of column collapse and PDC formation (i.e., conduit radius, wall-rock abundance, and magma discharge rate variations) with other properties linked to magma ascent (i.e., clast density, vesicle number density) that we measured. As suggested by Wilson et al. (1980), increases in MDR can lead to diminished air entrainment and mixing efficiency, and potentially explain the shift from dominantly convective to collapsing plumes. Based on column height calculations, Carey and Sigurdsson (1987) derived MDR values that increase from ~7 × $10^6$ kg $s^{-1}$ during EU2 to ~1.5 × $10^8$ kg $s^{-1}$ prior to P2 (Fig. 3A; Table DR3). During this eruptive interval, calculated decompression rates also increase in a comparable fashion. After P2, column heights calculated from inter-PDC fall units decreased, and so did the values of MDR. Therefore, PDCs were also produced at times of decreasing MDR, implying that other factors combined to destabilize the eruptive column. It is interesting that magma decompression rates just below the fragmentation level stay rather constant (or slightly increase) even if MDR values start to decrease. In fact, maximum $dP/dt$ values are calculated for P5, which was produced during a phase of lower magma discharge (<$10^7$ kg $s^{-1}$; Fig. 3A). Thus, the decrease in MDR from P2 to P5 did not originate from a change in ascent or decompression dynamics, but rather from a shift in the conduit and/or vent geometry.

For several eruptions, including Vesuvius A.D. 79, Kaminski and Jaupart (2001) proposed a model in which collapsing column regimes could be achieved if a non-negligible amount of gas was still trapped as unconnected bubbles within pumice clasts during fragmentation and therefore did not participate in the gas budget injected into the rising plume. New measurements of bubble connectivity through He-pycnometry (see Table DR1) on both fall and PDC pumice from the A.D. 79 eruption show that trapped bubbles did not form a significant fraction of the total vesicularity. As a result, it is unlikely that modifications in the exsolved volatile budget throughout this eruption made a strong enough impact on the plume to trigger its collapse.

Overall, several triggers for column destabilization, each linked to changes in wall rock or juvenile clast density, can be considered for the generation of PDCs during the A.D. 79 eruption.

### Trigger A. Increases in Juvenile Clast Density: Transitions From Fall Phases to Partial Collapses P1–P4

Compared to the fall samples that precede them, partial collapses P1–P4 all contain denser clasts on average (Fig. 3C). An increase in the proportion of dense clasts could have altered the dynamics of the convectively rising plume, and caused the passage from a stable to a partially collapsing column.

### Trigger B. Conduit Erosion and Increases in the Abundance of Wall Rock Within the Plume: Total Collapse P5

In contrast to partial collapse phases, pumice clasts sampled within P5 have densities only slightly higher than most of fall samples (Fig. 3C).

Inferred MDR values are lower than during previous gray magma phases, while decompression rates stabilize or slightly increase from P3 to P5, and reach the maximum value calculated (~13 MPa $s^{-1}$; Fig. 3A). As decompression rates remained approximately constant and the discharge rate was decreasing, erosion of conduit walls caused the incorporation of additional dense wall-rock material into the plume. Increasing vent radius possibly generated an increase in the lateral extent of the jet region at the base of the eruptive column, which limited the ability of the hot ejecta to mix efficiently with the atmosphere. Thus, both deep incorporation of conduit wall rock and vent widening could have promoted the total collapse of the eruptive column. The influence of wall rocks on the thermal budget of the plume was very minor in comparison, since most wall rocks from the conduit walls were preheated by the ascending magma before being incorporated in the eruptive mixture (Cioni et al., 2004).

### Trigger C. Increases in Juvenile Clast Density Combined With Conduit Widening and Increases in the Wall-Rock Content: Generation of P6

P6 was generated after the total column collapse phase and contains the highest fraction of dense juvenile clasts measured (cf. Fig. 3C). The exceptionally high wall-rock content of this deposit (64–72 vol%; Fig. 3B; Table DR2) implies that by P6 time, the conduit had widened significantly, though MDR was waning (Fig. 3A). Decompression rates calculated for this unit are still elevated (4 MPa $s^{-1}$), but represent the lowest values measured in all PDC samples. Thus, the high content of dense juvenile clasts and wall rocks coupled with the enlarged conduit probably combined to generate a low, fully collapsing low-energy plume resulting in a PDC that was rapidly channeled by the topography and that traveled short distances from the vent (Cioni et al., 2004).

## WHAT CAUSED VARIATIONS IN THE ABUNDANCE OF DENSE JUVENILE CLASTS DURING THE ERUPTION?

Peaks in proportions of dense clasts occurred during five out of the six transitions from fall to PDC-producing columns (P5 being the exception). Assuming that pumice textures from this eruption were frozen at or near fragmentation (e.g., Gurioli et al., 2005), the processes responsible for the increase in density likely took place within the conduit, and were intimately linked to degassing. To date, no detailed model accounts for systematic spatial gradients in vesicularity (and thereby density) across and along volcanic conduits. Sable et al. (2006) suggested that velocity gradients across ascending magma should cause spatial variations in the extent of degassing due to contrasting residence times in the conduit. How such gradients may vary temporally during the course of an entire eruption remains unclear. What are the conduit conditions that lead to fluctuating proportions of dense versus lighter pumice at fragmentation? This question can be addressed through a detailed textural comparison of products from both PDC and fall phases.

## CONCLUSIONS

The study of pyroclasts within six PDC deposits from the A.D. 79 eruption revealed that stable to collapsing column transitions coincide with peaks in the abundance of dense juvenile and wall-rock clasts. At least four partial collapses (P1–P4) resulted from increases in the abundance of denser pumice. In turn, the conditions leading to total collapse P5 were probably favored by the widening of the conduit system and the ensuing increase in the abundance of wall rock injected into the plume. The last small-scale collapse of the magmatic phase (P6) occurred when discharge rates were low, but the extremely high clast densities combined with the enlarged conduit led to the formation of a boil-over collapse. This study illustrates that, in order to effectively model column behavior during explosive eruptions, several transient parameters need to be accounted for. While recent plume models account for increasingly complex input variables such as particle size distributions, the variations of particle density have yet to be included. Future models involving the effects of particle density and vesicularity may also elucidate the causes for column collapse in other volcanic settings.


## ACKNOWLEDGMENTS

We acknowledge National Science Foundation grant EAR-0537950. J. Larsen, A. Harris, and M. Polacci helped with sample collection. We thank three anonymous reviewers.


## REFERENCES CITED


Barberi, F., Cioni, R., Rosi, M., Santacroce, R., Sbrana, A., and Vecci, R., 1989, Magmatic and phreatomagmatic phases in explosive eruptions of Vesuvius as deduced by grain-size and compositional analysis of pyroclastic deposits: Journal of Volcanology and Geothermal Research, v. 38, p. 287–307, doi:10.1016/0377-0273(89)90044-9.

Carey, S., and Sigurdsson, H., 1987, Temporal variations in column height and magma discharge rate during the A.D. 79 eruption of Vesuvius: Geological Society of America Bulletin, v. 99, p. 303–314, doi:10.1130/0016-7606(1987)99<303:TVICHA>2.0.CO;2.

Cioni, R., Marianelli, P., and Sbrana, A., 1992, Dynamics of the AD 79 eruption: Stratigraphic, sedimentological and geochemical data on the successions from the Somma-Vesuvius southern and eastern sectors: Acta Vulcanologica, v. 2, p. 109–123.

Cioni, R., Gurioli, L., Lanza, R., and Zanella, E., 2004, Temperatures of A.D. 79 pyroclastic density currents deposits (Vesuvius, Italy): Journal of Geophysical Research, v. 109, B02207, doi:10.1029/2002JB002251.

Clarke, A., Voight, B., Neri, A., and Macedonio, G., 2002, Transient dynamics of vulcanian explosions and column collapse: Nature, v. 415, p. 897–901, doi:10.1038/415897a.

Gurioli, L., Cioni, R., Sbrana, A., and Zanella, E., 2002, Transport and deposition from pyroclastic flows over an inhabited area: The deposits of the AD 79 eruption of Vesuvius at Herculaneum, Italy: Sedimentology, v. 49, p. 929–953, doi:10.1046/j.1365-3091.2002.00483.x.

Gurioli, L., Houghton, B.F., Cashman, K.V., and Cioni, R., 2005, Complex changes in eruption dynamics during the 79 AD eruption of Vesuvius: Bulletin of Volcanology, v. 67, p. 144–159, doi:10.1007/s00445-004-0368-4.

Kaminski, E., and Jaupart, C., 2001, Marginal stability of atmospheric eruption columns and pyroclastic flow generation: Journal of Geophysical Research, v. 106, no. B10, doi:10.1029/2001JB000215.

Lirer, L., Pescatore, T., Booth, B., and Walker, G.P.L., 1973, Two Plinian pumice-fall deposits from Somma-Vesuvius, Italy: Geological Society of America Bulletin, v. 84, p. 759–772, doi:10.1130/0016-7606(1973)84<759:TPPDFS>2.0.CO;2.

Mastin, L.G., and Ghiorso, M.S., 2000, A numerical program for steady-state flow of magma-gas mixtures through vertical eruptive conduits: U.S. Geological Survey Open-File Report 00–209, 61 p.

Neri, A., Papale, P., Del Seppia, D., and Santacroce, R., 2003, Coupled conduit and atmospheric dispersal dynamics of the AD 79 Plinian eruption of Vesuvius: Journal of Volcanology and Geothermal Research, v. 120, p. 141–160, doi:10.1016/S0377-0273(02)00381-5.

Sable, J.E., Houghton, B.F., Del Carlo, P., and Coltelli, M., 2006, Changing conditions of magma ascent and fragmentation during the Etna 122 BC basaltic Plinian eruption: Evidence from clast microtextures: Journal of Volcanology and Geothermal Research, v. 158, p. 333–354, doi:10.1016/j.jvolgeores.2006.07.006.

Shea, T., Houghton, B.F., Gurioli, L., Cashman, K.V., Hammer, J.E., and Hobden, B., 2010a, Textural studies of vesicles in volcanic rocks: An integrated methodology: Journal of Volcanology and Geothermal Research, v. 190, p. 271–289, doi:10.1016/j.jvolgeores.2009.12.003.

Shea, T., Gurioli, L., Larsen, J.F., Houghton, B.F., Hammer, J.E., and Cashman, K.V., 2010b, Linking experimental and natural vesicle textures in Vesuvius 79AD white pumice: Journal of Volcanology and Geothermal Research, v. 192, p. 69–84, doi:10.1016/j.jvolgeores.2010.02.013.

Toramaru, A., 2006, BND (bubble number density) decompression rate meter for explosive volcanic eruptions: Journal of Volcanology and Geothermal Research, v. 154, p. 303–316, doi:10.1016/j.jvolgeores.2006.03.027.

Wilson, L., Sparks, R.S.J., and Walker, G.P.L., 1980, Explosive volcanic eruptions—IV. The control of magma properties and conduit geometry on eruption column behavior: Royal Astronomical Society Geophysical Journal, v. 63, p. 117–148.



Manuscript received 19 January 2011
Manuscript accepted 2 March 2011

Printed in USA